TNFRSF14 (HVEM) is a novel immune checkpoint blockade that can be targeted by a monoclonal antibody to improve anti-tumor response in humanized mice

Brunel S.[1*], Aubert N. [1*], Olive D.[2] and Marodon G.[1]

1 Sorbonne Universités, Inserm, CNRS, Centre d'immunologie et maladies infectieuses-Paris, Cimi-Paris, Paris 75013, France
2 Institut Paoli-Calmettes, Aix-Marseille Université, Inserm, CNRS, CRCM, Tumor Immunity Team, IBISA Immunomonitoring platform, Marseille, France

* Equal contributions

Corresponding author: Gilles Marodon gilles.marodon@inserm.fr, Sorbonne Universités, Inserm, CNRS, Centre d'immunologie et maladies infectieuses-Paris, Cimi-Paris, Paris 75013, France

Abstract

Background: The TNFRSF14 (herpes virus entry mediator (HVEM)) delivers a negative signal to T cells through the B and T Lymphocyte Attenuator (BTLA) molecule and has been associated to a worse prognosis in various malignancies. Here, we investigated whether HVEM might represent a novel target for cancer immunotherapy.
Methods: To establish that HVEM represents a novel immune checkpoint, we compared the growth of a prostate cancer cell line expressing or rendered deficient for HVEM by CRISPR/Cas9 genetic editing in PBMC-humanized NOD.SCID.gamma.c-null (NSG) mice. A murine monoclonal antibody to human HVEM was then used to assess the impact of inhibiting the HVEM/BTLA immune checkpoint on tumor growth. We also investigated the mode of action of the antibody by monitoring *in vitro* its impact on tumor growth and cell viability. We used non parametric t-tests, linear and non linear regression modeling to assess statistical significance of our results.
Results: We show that deleting HVEM or blocking HVEM/BTLA with a mAb has a profound impact on tumor growth in mice reconstituted with human T cells. This was associated with an increase in the proliferation and number of TIL. However, the

therapeutic effect of the mAb was lost with the tumor deficient for HVEM, showing that HVEM expression by the tumor was necessary for the therapeutic effect. Accordingly, no agonist activity of the mAb was detected on human T cells *in vivo*. Surprisingly, we observe a similar albeit milder effect of the antibody on tumor growth in non-humanized NSG mice that is also lost with the HVEM-deficient cell line. However, *in vitro* analyses show that the antibody alone has no significant impact on tumor survival *per se.* In contrast, addition of peritoneal macrophages from NSG mice to the culture results in higher mortality of the tumor, suggesting that myeloid cells of NSG mice might participate in tumor control *in vivo*. Finally, we reproduce the *in vivo* anti-tumor effect of the antibody with an HVEM-positive human melanoma cell line, but not with an HVEM-negative human breast cancer cell line, suggesting that the therapy could be applied to various HVEM-positive cancers, independently of their tissue origin.

Conclusion: Our results show that HVEM/BTLA is a novel immune checkpoint and that a mAb targeting HVEM might be a promising strategy for cancer immunotherapy.

Keywords

immune checkpoint; HVEM; BTLA; monoclonal antibody; cancer immunotherapy; humanized mice

Background

Immune escape by tumor is now considered a hallmark of cancer (1). Many immune mechanisms are involved to explain loss of tumor control, including defective MHC function and expression, recruitment of suppressive immune cells or expression of co-inhibitory receptors such as PD-L1 (2). In the last few years, targeting co-inhibitory molecules (that can be expressed by tumor or immune cells) with antibodies showed impressive results in tumor regression and overall survival, leading to approval of anti-CTLA-4, anti-PD-1 and anti-PD-L1 in numerous cancers (3). However, the success of immune checkpoint inhibitors (ICI) is still partial and many patients fail to respond. Limited tumor infiltrate (cold tumors) or low expression of the targeted molecule may explain the relative inefficiency of ICI (4,5). To overcome these limitations, it is necessary to explore other pathways that might be involved in immune escape and that could complement actual therapies.

Recently, a new co-inhibitory pair has been highlighted in anti-tumor immune response: HVEM (Herpes Virus Entry Mediator, TNFRSF14) and BTLA (B and T

lymphocyte attenuator). These two molecules can be expressed by many immune cells including T-cells, in which signaling through BTLA is associated to inhibition of their activation (6,7). Additionally, the HVEM network includes many additional partners, such as LIGHT, lymphotoxin α (LTα) or CD160 (8). Like BTLA, binding of HVEM to CD160 on T-cells is associated with an inhibition of their activation (9). On the other side, stimulation of HVEM on T-cells by any of its ligands is associated with proliferation, survival and inflammatory cytokines production, such as IL-2 and IFN-γ (9,10). Several clinical studies have shown that HVEM expression is upregulated in many types of cancers including colorectal cancers (11), esophageal carcinomas (12), gastric cancers (13), hepatocarcinomas (14), breast cancers (15) or lymphomas (16). In these studies, high level of HVEM expression by tumors was associated with worse prognosis and lower survival. Moreover, HVEM expression by tumors was also associated with a reduction of CD4 and CD8 tumor-infiltrating lymphocytes (TIL) numbers (11,12,14).

Few studies considered affecting tumor growth by targeting the HVEM network. In fact, strategies to inhibit HVEM expression by tumors, by competing for its ligands or directly stimulating HVEM expressed on T-cells, lead to increased T cell proliferation and function in syngeneic mouse models (12,17–19). However, to our knowledge, no study so far has assessed the possibility to use a monoclonal antibody (mAb) to HVEM to favor the anti-tumor immune response and *a fortiori* in a humanized context *in vivo*. Herein, we explored the possibility that HVEM/BTLA might represent a novel immune checkpoint during anti-tumor immunity and investigate the therapeutic potential of a murine antibody targeting human HVEM in humanized mice models grafted with various human tumor cell lines, which express HVEM or engineered not to express HVEM by CRISPR/Cas9. To generate humanized mice, we used immuno-compromised NOD.SCID.γc^{null} (NSG) mice which are deprived of murine T-, B- and NK-cells but that retain functionally immature macrophages and multinucleated cells (20). We reconstituted these mice with human PBMC, allowing the effect of blocking HVEM to be studied on both tumors, murine myeloid cells and human T-cells. Our results indicate that HVEM/BTLA is a novel immune checkpoint that can be targeted with an anti-HVEM mAb, a potential useful strategy for cancer immunotherapy of HVEM$^+$ tumors.

Methods

Preparation of human peripheral mononuclear cells

Human peripheral blood mononuclear cells were isolated on a Ficoll gradient (Biocoll). Cells were washed in PBS 3% FCS and diluted at the appropriate concentration in 1× PBS before injection into mice.

Humanized mice tumor model

All animals used were NSG mice (stock ≠005557) purchased from the Jackson laboratory (USA). To assess therapeutic activity, 8–20-week-old NSG mice (males and females) were injected subcutaneously with 2.10^6 tumour cells. One week later, mice were irradiated (2 Gy) and engrafted the same day with 2.10^6 huPBMC by retro orbital injection. 4-5 days after transplantation, the anti-huHVEM antibody or isotype control was injected intraperitoneally at 2 mg/kg. General state, body weight and survival of mice were monitored every 3-4 days to evaluate Graft-vs-Host-Disease (GVHD) progression. Mice were euthanized when exhibiting signs of GVHD, such as hunched back, ruffled fur, and reduced mobility.

Antibodies

The clone 18.10 has been described previously (21). Briefly, 18.10 is a murine IgG1 anti-human HVEM mAb and was produced as ascites and purified by protein A binding and elution with the Affi-gel Protein A MAPS II Kit (Bio-rad). Mouse IgG1 isotype control (MOPC-21 clone) was purchased from Bio X Cell (West Lebanon, NH, USA).

Cell lines

PC3 (non-hormone-dependant human prostate cancer cells), Gerlach (human melanoma cells), MDA-MB-231 (breast cancer cells) were grown in high glucose DMEM media supplemented with 10% FCS, L-glutamine and antibiotics (Penicillin/Streptomycin). PC3 and MDA-MB-231 were genetically authenticated (Eurofins). All cells were confirmed to be free of mycoplasmas before injection into mice by the MycoAlert detection kit (Lonza). Tumor growth was monitored using an electronic calliper and volumes were determined using the following formula: $[(\text{length}*\text{width}^2)/2]$. The PC3-GFP cell line was generated in the laboratory by lentiviral transduction (details available on request).

Generation of HVEM deficient PC3 clone using CRISPR-Cas9 technology

50,000 PC3 cells were seeded in a 24-well plate. Twenty-four hours later, cells were incubated with sgRNA complementary to exon3 of HVEM (GCCAUUGAGGUGGGCAAUGU + Scaffold, TrueGuide Synthtetic guide RNAs, Invitrogen™), Cas9 nuclease (TrueCut™ Cas9 Protein v2, Invitrogen™) and lipofectamine (Lipofectamine™ CRISPRMAX™ Cas9 Transfection Reagent, Invitrogen™) according to manufacturer instructions (TrueCut Cas9 protein v2 (27/09/2017)). After three days, efficiency was evaluated with GeneArt Genomic Cleavage Detection Kit (Invitrogen™) according to the manufacturer instructions. For this assay, DNA was

amplified with the following primers: TGCGAAGTTCCCACTCTCTG (Forward) and GGATAAGGGTCAGTCGCCAA (Reverse). Cells were cloned by limiting dilution in 96-well plates. Clones were screened for HVEM expression by flow cytometry using anti-HVEM (clone 94801, BD) and were considered as negative if HVEM expression was undetectable for at least 3 subsequent measurements.

In vitro assays

PC3 cells were seeded in 96-wells plate at 7000 cells/well in RPMI medium. Macrophages from NSG mice were obtained by peritoneal wash. The target to effector ratio was 1:10 for cell death evaluation and 1:5 for apoptosis monitoring. Cells were treated by the anti HVEM antibody or its isotype control MOPC21 at 10µg/ml. Cell death was evaluated by flow cytometry after 16 hours of incubation (37°C, 5%CO2) by 7AAD staining. For live cell imaging, apoptosis of the PC3 GFP cell line was assessed using the annexin V red reagent for apoptosis (cat n°4641, Sartorius). Culture was monitored every hour during 16 hours by Incucyte and overlapping of GFP (green) and apoptosis staining (red) was quantified and reported as number of apoptotic cells/well.

Phenotypic analysis by flow cytometry

Tumors were digested with 0.84mg/mL of collagenase IV and 10µg/mL DNAse I (Sigma Aldrich) for 40min at 37°C with an intermediate flushing of the tissue. Cells were passed through a 100µm-cell strainer and resuspended in PBS 3% SVF. To eliminate dead cells and debris, tumor cell suspensions were isolated on a Ficoll gradient. Rings were collected, washed, and cell pellets were resuspended in PBS 3%SVF before counting on LUNA™ Automated Cell counter (Logos Biosystems). Subsequently, up to 2.10^6 live cells were stained with viability dye (eF506, Fixable Viability Dye, ThermoFisher) for 12min at 4°C, Fc receptor were blocked with human FcR Blocking Reagent (120-000-442, Miltenyi Biotec) and anti-CD16/32 (clone 2.4G2) for 10min. The followings antibodies were added for 35min at 4°C: hCD45-BUV805 (HI30, BD), hCD3-PECyn7 (SK7, BD), hCD4-PerCP (RPA-T4, Biolegend), hCD8-APC-H7 (SK1, BD), hKi67-AF700 (B56, BD), hCD270-BV421 (cw10, BD), and mCD45-BUV395 (30-F11, BD). For intracellular staining, Foxp3/Transcription Factor Staining Buffer Set (eBioscience) was used. Cells were washed with 1X PBS before acquisition on an X20 cytometer (Becton Dickinson (BD), San Jose, CA). The absolute count of different populations was determined by adding 50 µL of Cell Counting Beads (Bangs Laboratories) just before acquisition. Data were analyzed using FlowJo software (TreeStar, Ashland, OR, USA).

Statistical analysis

All statistical tests were performed with Prism software (Graph Pad Inc, La Jolla, CA, USA). To compare ranks between two groups, the p-value was calculated with a non-parametric two tailed Mann-Whitney t-test. Survival analyses were performed with a log-rank (Mantel-Cox) test. Statistical modelling of tumor growth was performed by linear and non-linear regression using the exponential growth model. The p-values of these tests are indicated on each panel. Statistical power of the analyses (alpha) was arbitrarily set at 0.05. No a priori test were performed to adequate the number of samples with statistical power.

Results

HVEM is an immune checkpoint during anti-tumor T cell immune response

To investigate whether HVEM might behave as an immune checkpoint for tumor control in humanized mice, we generated an HVEM-deficient cell line derived from HVEM-expressing PC3 cell line using CRISPR-Cas9 technology (Fig 1A). Transfection of CRISPR-Cas9/sgRNA complex resulted in 30% of cleavage efficiency, corresponding to 4% of cells affected on two alleles (Figure S1A). After subcloning, we obtained several clones with prolonged undetectable surface expression of HVEM (Figure S1B). We picked the clone 1B11 for further experiments given its morphological similarity with wild-type PC3 (Figure S1C). Although both cell lines grew similarly in non-humanized NSG mice, there was a marked difference in tumor growth in PBMC-reconstituted mice: HVEM-deficient PC3 1B11 grew slower compared to wild type PC3, demonstrating that HVEM acted like an immune checkpoint blocker in this model (Figure 1B).

Anti-HVEM treatment is associated to a reduction in tumor growth and an increase in TIL number and proliferation that depend on HVEM expression by the tumor

Having demonstrated that HVEM was an immune checkpoint for anti tumor immunity, we wanted to evaluate whether HVEM could be targeted for therapy by a monoclonal antibody. Thus, NSG mice were grafted s.c with parental PC3 or the HVEM-deficient 1B11 clone, injected with PBMCs from healthy donors 7 to 8 days after and treated weekly with 2mg/kg of the 18.10 anti-HVEM mAb. Tumor growth was significantly reduced in mice treated with the 18.10 mAb compared to isotype-treated controls, an effect that could already be observed after a single injection (Figure 2A). Flow cytometry analysis of human tumor-infiltrating lymphocytes (TIL) revealed an increase in CD4 T-cells numbers and a similar tendency for CD8 T-cells (Figure 2B). Additionally, frequencies of cells expressing the proliferation marker Ki67 were significantly

elevated in both CD4 and CD8 T-cells (Figures 2C). However, the treatment with the anti-HVEM mAb was ineffective at controlling the growth of 1B11 in humanized mice (Figure 2D), indicating an essential role for HVEM expressed by the tumor in treatment efficacy. Accordingly, no difference in TIL numbers (Figure 2E) or frequencies of Ki-67$^+$ T cells (Figure 2F) could be detected with the HVEM-deficient PC3 cell line. Overall, anti-HVEM therapy in humanized mice decreased the growth of the PC3 cell line, associated to an increase in TIL numbers and proliferation that depend on HVEM expression by the tumor.

The mAb has no direct effect on human T cells *in vivo*

We monitored HVEM expression by human PBMC and confirmed that HVEM was highly expressed by human T and B cells before injection into mice (Figure 3A). Thus, the data described above could be explained in part by activation of the HVEM signaling pathway, leading to improved proliferation and functions of human T cells *in vivo*. Several lines of evidence argue against this hypothesis. First, the number and proliferation status of TIL was not affected by the treatment in the absence of tumor control (Fig 2C-D). Second, Graft-vs-Host Disease (GVHD) that occurs in immuno-compromised mice grafted with human T cells, was not affected by the treatment as documented by similar weight loss and survival in the experimental groups (Fig 3B). Third, similar numbers and frequencies of Ki67$^+$ cells were observed in the spleens of mice of HVEM-treated or control groups (Figures 3C). Altogether, these results show that the mAb has no effect on human T cells *in vivo*, at least in this humanized mice model.

NSG myeloid cells are able to kill wild-type PC3 cells in presence of anti-HVEM antibody

Knowing that HVEM expression by the tumor was crucial for the efficacy of the mAb, and that it had no direct impact on human T cells *in vivo*, we evaluated whether the mAb would be able to mediate killing of tumor cells. To that end, we engrafted PC3 wild-type and clone 1B11 in non-humanized NSG mice and monitored tumor growth following mAb administration. Interestingly, a significant reduction in tumor growth was observed for wild-type PC3 (Figure 4A). In contrast, no difference in tumor growth was observed for the clone 1B11 with anti-HVEM therapy (Figure 4B). Thus, the mAb had a mild toxic effect on the cell line in the absence of human T cells, suggesting a direct effect mediated by HVEM signaling on the tumor. However, *in vitro* assays showed that the anti-HVEM mAb was unable to induce tumor cell death by itself (Figure 4C). Because NSG mice are on a NOD genetic background which is deficient for complement activity (20), we surmised that innate immunity of NSG mice might be

involved in the activity of the mAb. To assess the participation of myeloid cells in the anti-tumor response, we injected the anti-Gr1 mAb during the anti-HVEM treatment to deplete neutrophils and macrophages of NSG mice. There was a trend for an abolition of the effect of the HVEM mAb in anti-Gr1-treated mice compared to controls (Figure S2C), suggesting that $Gr1^+$ cells might participate in tumor control following treatment. However, NSG mice treated with anti-Gr1 rapidly suffered weight loss and died (Figure S2A-B), obscuring the interpretations of these experiments. To bypass this difficulty, we cultured PC3 cells with peritoneal cells from NSG mice, which were mostly macrophages (Figure S3). This resulted in an increased proportion of apoptotic cells in the culture in presence of the anti-HVEM mAb, using live imaging (Figure 3D). Furthermore, examination of video microscopy of the co-cultures revealed that tumor cells were killed by contact with NSG peritoneal macrophages with no evidence for engulfment of tumor cells (Video S1). Altogether, these results show that NSG peritoneal macrophages were able to kill HVEM-expressing tumor cells in presence of the anti-HVEM mAb by a cell-contact dependent mechanism.

Anti-HVEM anti-tumor effect in melanoma but not triple-negative breast cancer in humanized mice

In light of the effect of the anti-HVEM mAb on PC3 tumor growth, we sought to determine whether this observation could be extrapolated to other type of tumors. No difference in tumor growth were observed with mice grafted with the triple-negative breast cancer cell line MDA-MB-231, which does not express HVEM (Figure 5A-B). In contrast, a significant reduction of tumor growth was observed in mice grafted with the HVEM-positive Gerlach melanoma cell line (Figure 5C-D), similar to the PC3 cell line. Thus, therapeutic efficacy of the anti-HVEM mAb was heavily dependent on the expression of HVEM by the tumor rather than by the tissue origin of the tumor.

Discussion

Here, we report for the first time that HVEM is a novel immune checkpoint during anti-tumor immunity in humanized mice. This property led us to test the efficacy of anti-HVEM therapy in humanized mice in various tumor models. Targeting HVEM with an antibody may possibly acts on tumor growth through four non-mutually exclusive mechanisms in our model: (i) blockade of the interaction between tumor HVEM and its ligands expressed on immune cells (especially BTLA and CD160 for T-cells) should nullify inhibition of T-cell activation and consequently allow T-cell proliferation and possibly improved functions and tumor killing, (ii) stimulation of HVEM signaling on T-cells (agonist effect) by the mAb may promote their proliferation and functions to

enhance killing of tumor cells, (iii) stimulation of HVEM signaling in tumor may also promote tumor cell death directly, as it has been reported that in some circumstances HVEM signaling may induce apoptosis (22), and (iv) immunogenic tumor cell death may be caused by FcR-dependent mechanisms elicited by murine myeloid cells (23).

Here, we have tested these hypotheses and found that the mAb was unable to directly activate human T cells, as judged by similar frequencies of $Ki67^+$ cells and GVHD occurrence in anti-HVEM treated mice relative to controls. Furthermore, we show that HVEM expression by the tumor was necessary to elicit tumor control by the mAb. However, we did not observe increased tumor killing *in vitro* in presence of the mAb relative to isotype control, indicating that direct killing *in vivo* might not be the chief mechanism that can explain tumor control by the mAb. Surprisingly, we identified myeloid cells of NSG mice as key players in the mode of action of the mAb, confirming published observations in syngeneic mouse models that myeloid cells are crucial for tumor control upon immune checkpoints inhibitors treatment (24–26). NSG mice have no T-cells, no B-cells, no NK-cells owing to the SCID and γc mutations, and no complement and defectives DC and macrophages owing to the NOD genetic background (27). Here, we showed that killing of tumor cells by peritoneal macrophages from NSG mice was enhanced in presence of the anti-HVEM mAb, providing a possible mechanism to explain better control of tumor growth *in vivo* with or without human T cells. Because of the murine nature of the mAb, binding to murine Fc-receptors present on myeloid cells of NSG might have propelled the therapeutic efficacy of the mAb. In our setting, we used IgG1, that is reported to bind to CD16 (FcgRIII) and CD32 (FcgRIIB), activating and inhibitory receptors, respectively (28). However, NOD background has been associated with a strong decrease in FcgRIIB expression by macrophages (29). Consequently, activating FcgRIII might be the main receptor involved in FcR-dependent activity of murine myeloid cells in NSG mice. Several possibilities exist to explain tumor killing by myeloid cells, through antibody-dependent cellular phagocytosis (ADCP), local secretion of cytokines or free radicals, expression of FasL that would target Fas expressed by tumor cells and many others (30,31). We did not see evidence for ADCP on the video microscopies collected during the course of this study, which rather indicated that cell killing was mediated by cell contact. The exact mechanism by which myeloid cells killed the tumor in presence of the mAb remains to be elucidated.

An important observation that we made using CRISPR/Cas9 abolition of HVEM expression, was that the expression of HVEM by the tumor was strictly required for therapeutic efficacy. Thus, one can infer that HVEM expression by human cells play little or no role in our model. In contrast, Park *et al.* showed in a syngeneic mouse model that transfecting an agonist scFv anti-HVEM on tumors cells resulted in an

increase in T-cell proliferation, as well as improved IFN-γ and IL-2 production and better tumor control (18). This discrepancy could be explained by the fact that T-cells are strongly activated in huPBMC mice (32). Since HVEM is downregulated upon activation (33), it may have limited binding of anti-HVEM antibody on T-cells in our model. Thus, it remains possible that the mAb is still endowed with agonist properties *in vitro* or that it would behave differently in another model or in humans. On the other side, BTLA is also upregulated upon T-cell activation (33), so the anti-HVEM mAb might also have limited inhibition of activated T-cells through inhibition of the HVEM-BTLA axis. Indeed, we observed improved rejection of the HVEM-deficient tumor by human T cells relative to the wild type tumor, indicating that the HVEM/BTLA signaling is inhibitory for anti-tumor immunity in humanized mice. Likewise, previous studies in mice showed that inhibiting HVEM expression on the tumor or its interaction with its ligands has a positive effect on T cells. Injection of a plasmid encoding a soluble form of BTLA (to compete with endogenous BTLA for HVEM) was associated with an increase inflammatory cytokines production by TIL and a decrease in anti-inflammatory cytokines at the RNA level (17). Moreover, silencing of tumor HVEM with siRNA was also associated with an increase in CD8 T cells and inflammatory cytokine production in a murine colon carcinoma model (12). In addition, use of siRNA to HVEM on ovarian cancer *in vitro* promote T-cells proliferation and TNF-α and IFN-γ (19). Thus, our data suggest the following model to explain the anti-tumor activity of our anti-HVEM antibody in NSG mice: binding of the mAb on HVEM expressed by the tumor would activate tumor killing by murine myeloid cells, which together with blockade of the HVEM inhibitory network would enhance proliferation and functions of human T-cells to kill tumor cells.

Scheduled treatment with an anti-human HVEM mAb in humanized mice exerted a potent anti-tumor effect on the two HVEM-positive tumor cell lines tested, opening the possibility to apply this therapy to a wide range of solid cancers where HVEM is over expressed (11–15,34–39). The recent success of ICI for cancer immunotherapy (anti-CTLA-4, anti-PD-1/PD-L1) has confirmed the hypothesis that the immune system can control many cancers. In light of the promising results reported herein, anti-HVEM therapy might be combined with ICI to further enhance anti-tumor immunity.

Conclusions

Our study provides the first proof-of-concept that targeting HVEM is a new strategy for cancer immunotherapy. This is supported by data generated in humanized mice, carrying human tumors and human T cells, improving the relevance of our results relative to murine syngeneic models.

Abbreviations

HVEM, Herpes Virus Entry Mediator; BTLA, B and T Lymphocyte Attenuator; TNFRSF, Tumor Necrosis Factor Receptor Superfamily; NSG, NOD.SCID.γc^{null}; monoclonal antibody, mAb; ADCP, Antibody Dependent Cellular Phagocytosis; ICI, Immune Checkpoint Inhibitors

Declarations

Ethics approval and consent to participate

Human peripheral blood mononuclear cells were collected by Etablissement Français du Sang from healthy adult volunteers after informed consent in accordance with the Declaration of Helsinki. Mice were bred in our animal facility under specific pathogen-free conditions in accordance with current European legislation. All protocols were approved by the Ethics Committee for Animal Experimentation Charles Darwin (Ce5/2012/025).

Consent for publication: Not applicable

Availability of data and materials: the datasets used and/or analysed during the current study are available from the corresponding author on reasonable request.

Competing interests: D.O. is cofounder and a shareholder of Imcheck Therapeutics.

Funding

This study was supported by INSERM Transfert, Cancéropôle Île-de-France and Association pour la recherche sur les tumeurs de la prostate (ARTP). The funders play no role in the design of the study and collection, nor in the analysis or interpretation of the data. S.B. was supported by a doctoral fellowship from the French Ministère de l'Education Supérieure et de la Recherche. N.A. is supported by a doctoral fellowship from the Fondation ARC pour la recherche sur le cancer. D.O.'s team was supported by the grant "Equipe FRM DEQ201802339209". D.O. is Senior Scholar of the Institut Universitaire de France.

Authors' contributions

SB and NA performed the experiments, analyzed the data and contributed to the writing of the manuscript, DO provided essential reagents and edited the manuscript, GM designed the study, analyzed the data and wrote the manuscript. All authors read and approved the final manuscript.

Acknowledgments

The authors would like to thank Olivier Bregerie and Doriane Foret for taking care of our animal facility, Dr Pukar KC for technical help, and Dr Benoit Salomon for critical reading of the manuscript.

References

1. Hanahan D, Weinberg RA. Hallmarks of cancer: the next generation. Cell. 2011 Mar 4;144(5):646–74.

2. Mittal D, Gubin MM, Schreiber RD, Smyth MJ. New insights into cancer immunoediting and its three component phases — elimination, equilibrium and escape. Curr Opin Immunol. 2014 Apr;27:16–25.

3. Hargadon KM, Johnson CE, Williams CJ. Immune checkpoint blockade therapy for cancer: An overview of FDA-approved immune checkpoint inhibitors. International Immunopharmacology. 2018 Sep 1;62:29–39.

4. Havel JJ, Chowell D, Chan TA. The evolving landscape of biomarkers for checkpoint inhibitor immunotherapy. Nature Reviews Cancer. 2019 Mar;19(3):133.

5. Park Y-J, Kuen D-S, Chung Y. Future prospects of immune checkpoint blockade in cancer: from response prediction to overcoming resistance. Experimental & Molecular Medicine. 2018 Aug 22;50(8):109.

6. Cai G, Anumanthan A, Brown JA, Greenfield EA, Zhu B, Freeman GJ. CD160 inhibits activation of human $CD4^+$ T cells through interaction with herpesvirus entry mediator. Nature Immunology. 2008 Feb;9(2):176–85.

7. Sedy JR, Gavrieli M, Potter KG, Hurchla MA, Lindsley RC, Hildner K, et al. B and T lymphocyte attenuator regulates T cell activation through interaction with herpesvirus entry mediator. Nature Immunology. 2005 Jan;6(1):90.

8. Pasero C, Speiser DE, Derré L, Olive D. The HVEM network: new directions in targeting novel costimulatory/co-inhibitory molecules for cancer therapy. Current Opinion in Pharmacology. 2012 Aug 1;12(4):478–85.

9. Cheung TC, Steinberg MW, Oborne LM, Macauley MG, Fukuyama S, Sanjo H, et al. Unconventional ligand activation of herpesvirus entry mediator signals cell survival. Proc Natl Acad Sci USA. 2009 Apr 14;106(15):6244–9.

10. Harrop JA, McDonnell PC, Brigham-Burke M, Lyn SD, Minton J, Tan KB, et al. Herpesvirus entry mediator ligand (HVEM-L), a novel ligand for HVEM/TR2, stimulates proliferation of T cells and inhibits HT29 cell growth. J Biol Chem. 1998 Oct 16;273(42):27548–56.

11. Inoue T, Sho M, Yasuda S, Nishiwada S, Nakamura S, Ueda T, et al. HVEM Expression Contributes to Tumor Progression and Prognosis in Human Colorectal Cancer. Anticancer Res. 2015 Jan 3;35(3):1361–7.

12. Migita K, Sho M, Shimada K, Yasuda S, Yamato I, Takayama T, et al. Significant involvement of herpesvirus entry mediator in human esophageal squamous cell carcinoma. Cancer. 2014;120(6):808–17.

13. Lan X, Li S, Gao H, Nanding A, Quan L, Yang C, et al. Increased BTLA and HVEM in gastric cancer are associated with progression and poor prognosis. Onco Targets Ther. 2017 Feb 16;10:919–26.

14. Hokuto D, Sho M, Yamato I, Yasuda S, Obara S, Nomi T, et al. Clinical impact of herpesvirus entry mediator expression in human hepatocellular carcinoma. European Journal of Cancer. 2015 Jan 1;51(2):157–65.

15. Tsang JYS, Chan K-W, Ni Y-B, Hlaing T, Hu J, Chan S-K, et al. Expression and Clinical Significance of Herpes Virus Entry Mediator (HVEM) in Breast Cancer. Ann Surg Oncol. 2017 Dec 1;24(13):4042–50.

16. M'Hidi H, Thibult M-L, Chetaille B, Rey F, Bouadallah R, Nicollas R, et al. High Expression of the Inhibitory Receptor BTLA in T-Follicular Helper Cells and in B-Cell Small Lymphocytic Lymphoma/Chronic Lymphocytic Leukemia. Am J Clin Pathol. 2009 Oct 1;132(4):589–96.

17. Han L, Wang W, Fang Y, Feng Z, Liao S, Li W, et al. Soluble B and T Lymphocyte Attenuator Possesses Antitumor Effects and Facilitates Heat Shock Protein 70 Vaccine-Triggered Antitumor Immunity against a Murine TC-1 Cervical Cancer Model In Vivo. The Journal of Immunology. 2009 Dec 15;183(12):7842–50.

18. Park J-J, Anand S, Zhao Y, Matsumura Y, Sakoda Y, Kuramasu A, et al. Expression of anti-HVEM single-chain antibody on tumor cells induces tumor-specific immunity with long-term memory. Cancer Immunol Immunother. 2012 Feb 1;61(2):203–14.

19. Zhang T, Ye L, Han L, He Q, Zhu J. Knockdown of HVEM, a Lymphocyte Regulator Gene, in Ovarian Cancer Cells Increases Sensitivity to Activated T Cells [Internet]. 2016 [cited 2018 Dec 13]. Available from: https://www-ingentaconnect-com.gate2.inist.fr/content/cog/or/2016/00000024/00000003/art00007#

20. Shultz LD, Schweitzer PA, Christianson SW, Gott B, Schweitzer IB, Tennent B, et al. Multiple defects in innate and adaptive immunologic function in NOD/LtSz-scid mice. The Journal of Immunology. 1995 Jan 1;154(1):180–91.

21. Gertner-Dardenne J, Fauriat C, Orlanducci F, Thibult M-L, Pastor S, Fitzgibbon J, et al. The co-receptor BTLA negatively regulates human Vg9Vd2 T-cell proliferation: a potential way of immune escape for lymphoma cells. 2013;122(6):11.

22. Costello RT, Mallet F, Barbarat B, Schiano de Colella J-M, Sainty D, Sweet RW, et al. Stimulation of non-Hodgkin's lymphoma via HVEM: an alternate and safe way to increase Fas-induced apoptosis and improve tumor immunogenicity. Leukemia. 2003 Dec;17(12):2500–7.

23. Bakema JE, van Egmond M. Fc receptor-dependent mechanisms of monoclonal antibody therapy of cancer. Curr Top Microbiol Immunol. 2014;382:373–92.

24. Dhupkar P, Gordon N, Stewart J, Kleinerman ES. Anti-PD-1 therapy redirects macrophages from an M2 to an M1 phenotype inducing regression of OS lung metastases. Cancer Medicine. 2018;7(6):2654–64.

25. Gordon SR, Maute RL, Dulken BW, Hutter G, George BM, McCracken MN, et al. PD-1 expression by tumor-associated macrophages inhibits phagocytosis and tumor immunity. Nature. 2017 May 25;545(7655):495–9.

26. Gubin MM, Esaulova E, Ward JP, Malkova ON, Runci D, Wong P, et al. High-Dimensional Analysis Delineates Myeloid and Lymphoid Compartment Remodeling during Successful Immune-Checkpoint Cancer Therapy. Cell. 2018 Nov 1;175(4):1014-1030.e19.

27. Shultz LD, Lyons BL, Burzenski LM, Gott B, Chen X, Chaleff S, et al. Human Lymphoid and Myeloid Cell Development in NOD/LtSz-scid IL2Rγnull Mice Engrafted with Mobilized Human Hemopoietic Stem Cells. The Journal of Immunology. 2005 May 15;174(10):6477–89.

28. Bruhns P. Properties of mouse and human IgG receptors and their contribution to disease models. Blood. 2012 Jun 14;119(24):5640–9.

29. Luan JJ, Monteiro RC, Sautès C, Fluteau G, Eloy L, Fridman WH, et al. Defective Fc gamma RII gene expression in macrophages of NOD mice: genetic linkage with up-regulation of IgG1 and IgG2b in serum. J Immunol. 1996 Nov 15;157(10):4707–16.

30. Furness AJS, Vargas FA, Peggs KS, Quezada SA. Impact of tumour microenvironment and Fc receptors on the activity of immunomodulatory antibodies. Trends in Immunology. 2014 Jul 1;35(7):290–8.

31. Gül N, Egmond M van. Antibody-Dependent Phagocytosis of Tumor Cells by Macrophages: A Potent Effector Mechanism of Monoclonal Antibody Therapy of Cancer. Cancer Res. 2015 Dec 1;75(23):5008–13.

32. Ali N, Flutter B, Rodriguez RS, Sharif-Paghaleh E, Barber LD, Lombardi G, et al. Xenogeneic Graft-versus-Host-Disease in NOD-scid IL- 2Rcnull Mice Display a T-Effector Memory Phenotype. PLOS ONE. 2012;7(8):10.

33. Murphy KM, Nelson CA, Šedý JR. Balancing co-stimulation and inhibition with BTLA and HVEM. Nature Reviews Immunology. 2006 Sep;6(9):671–81.

34. Mochizuki K, Kawana S, Yamada S, Muramatsu M, Sano H, Kobayashi S, et al. Various checkpoint molecules, and tumor-infiltrating lymphocytes in common pediatric solid tumors: Possibilities for novel immunotherapy. Pediatr Hematol Oncol. 2019 Feb;36(1):17–27.

35. Ren S, Tian Q, Amar N, Yu H, Rivard CJ, Caldwell C, et al. The immune checkpoint, HVEM may contribute to immune escape in non-small cell lung cancer lacking PD-L1 expression. Lung Cancer. 2018 Nov 1;125:115–20.

36. Sideras K, Biermann K, Verheij J, Takkenberg BR, Mancham S, Hansen BE, et al. PD-L1, Galectin-9 and CD8+ tumor-infiltrating lymphocytes are associated with survival in hepatocellular carcinoma. OncoImmunology. 2017 Feb 1;6(2):e1273309.

37. Sideras K, Biermann K, Yap K, Mancham S, Boor PPC, Hansen BE, et al. Tumor cell expression of immune inhibitory molecules and tumor-infiltrating lymphocyte

count predict cancer-specific survival in pancreatic and ampullary cancer. International Journal of Cancer. 2017;141(3):572–82.

38. Tang M, Cao X, Li Y, Li G-Q, He Q-H, Li S-J, et al. High expression of herpes virus entry mediator is associated with poor prognosis in clear cell renal cell carcinoma. Am J Cancer Res. 2019 May 1;9(5):975–87.

39. Zhu Y-D, Lu M-Y. Increased expression of TNFRSF14 indicates good prognosis and inhibits bladder cancer proliferation by promoting apoptosis. Mol Med Rep. 2018 Sep;18(3):3403–10.

Figure legends

Figure 1: HVEM is a novel immune checkpoint blocker in humanized mice. (A-B) HVEM expression on PC3 wild type (WT) (A) and the PC3 1B11 subclone (1B11) (B) genetically modified by CRISPR/Cas9 was revealed with anti-HVEM mAb (clone 18.10) and a secondary antibody. Light peaks are the FMO controls. (C-D) Growth of the indicated PC3 cell lines (WT or 1B11) in non-humanized (C) or PBMC-humanized mice (D). Curves are the mean tumor volume (±SEM) in the indicated number of mice. Data are cumulative of at least two experiments. Statistical analysis was a linear regression model.

Figure 2: Treatment with the anti-HVEM mAb 18.10 is associated with a reduction of tumor growth and an increase in TIL number and proliferation. Growth of the PC3 wild type cell line (A) or the 1B11 PC3 subclone (D) grafted in humanized mice treated with anti-HVEM or isotype control (as described in material and methods). Curves are the mean tumor volume (±SEM) in the indicated number of mice. Data are cumulative of at least 2 independent experiments. Arrows indicate the time of injection. Statistical analysis was a linear regression model. Total number of $CD4^+$ and $CD8^+$ T-cells in PC3 wild type tumors (B) or in PC3 1B11 subclone (E) from one representative experiment out of 2. Numbers were determined by flow cytometry using Cell Counting Beads at day 18 post treatment initiation. Frequencies of Ki67-expressing cells among $CD4^+$ and $CD8^+$ T-cells in the PC3 wild type tumors (C) or the PC3 1B11 subclone (F). Data are cumulative of two independent experiments. Each dot is a mouse. Statistical significance was tested using the Mann-Witney non parametric t-test.

Figure 3: The HVEM mAb does not directly activate human T cells (A) Expression of HVEM on various subsets of PBMC before injection to mice (from 3 different donors). (B-C) Graft versus Host Disease is not affected by the HVEM mAb,

according to weight loss (B) or survival (C). Data are cumulative from 4 independent experiments. (D) Total number of $CD4^+$ and $CD8^+$ T-cells in the spleens from one representative experiment out of 2. Numbers were determined at day 23 post-humanization (E) Frequencies of Ki67-expressing cells among splenic $CD4^+$ and $CD8^+$ T-cells from two independent experiments.

Figure 4: NSG myeloid cells are able to kill wild-type PC3 cells in presence of the anti-HVEM antibody. Tumor growth of wild-type PC3 (WT) cell line (A) or the PC3 1B11 subclone (1B11) (B) in non-humanized NSG mice treated with the anti-HVEM mAb. Arrows indicate the time of injection. Data are cumulative of at least 2 experiments. (C) Frequencies of 7AAD+ cells of wild-type PC3 cells (WT) in culture with anti-HVEM or isotype control. (D) GFP-expressing wild-type PC3 cells were co-cultured with NSG peritoneal macrophages and an apoptosis staining reagent. Overlap of GFP (green) and apoptosis staining (red) was quantified and reported as number of apoptotic cells/well. Depicted are the results from one representative experiment out of two.

Figure 5: The anti-tumor effect of the anti-HVEM mAb is not restricted to the PC3 cell line. HVEM expression on MDA-MB-231 (MDA) (A) and Gerlach cells (C) revealed with anti-HVEM (clone 18.10) and secondary antibody. Tumor growth of MDA-MB-231 (B) and Gerlach (D) cell lines grafted in humanized mice treated with anti-HVEM (as described in material and methods). Curves represents the mean tumor volume (±SEM) from one experiment. Numbers of mice at the beginning of the experiment are indicated in brackets. Arrows indicate the time of the injections.

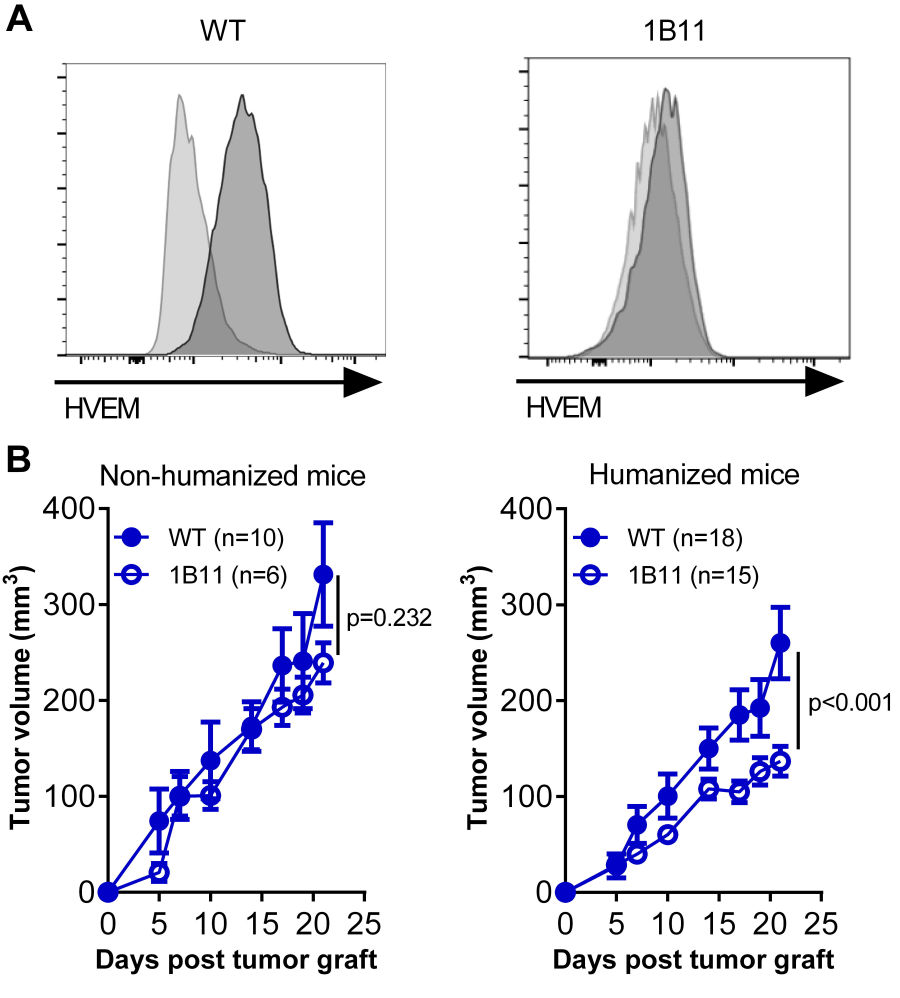
A
WT
1B11
HVEM
HVEM
B
Non-humanized mice
Humanized mice
WT (n=10)
1B11 (n=6)
p=0.232
WT (n=18)
1B11 (n=15)
p<0.001
Tumor volume (mm3)
Days post tumor graft
0
100
200
300
400
0
5
10
15
20
25

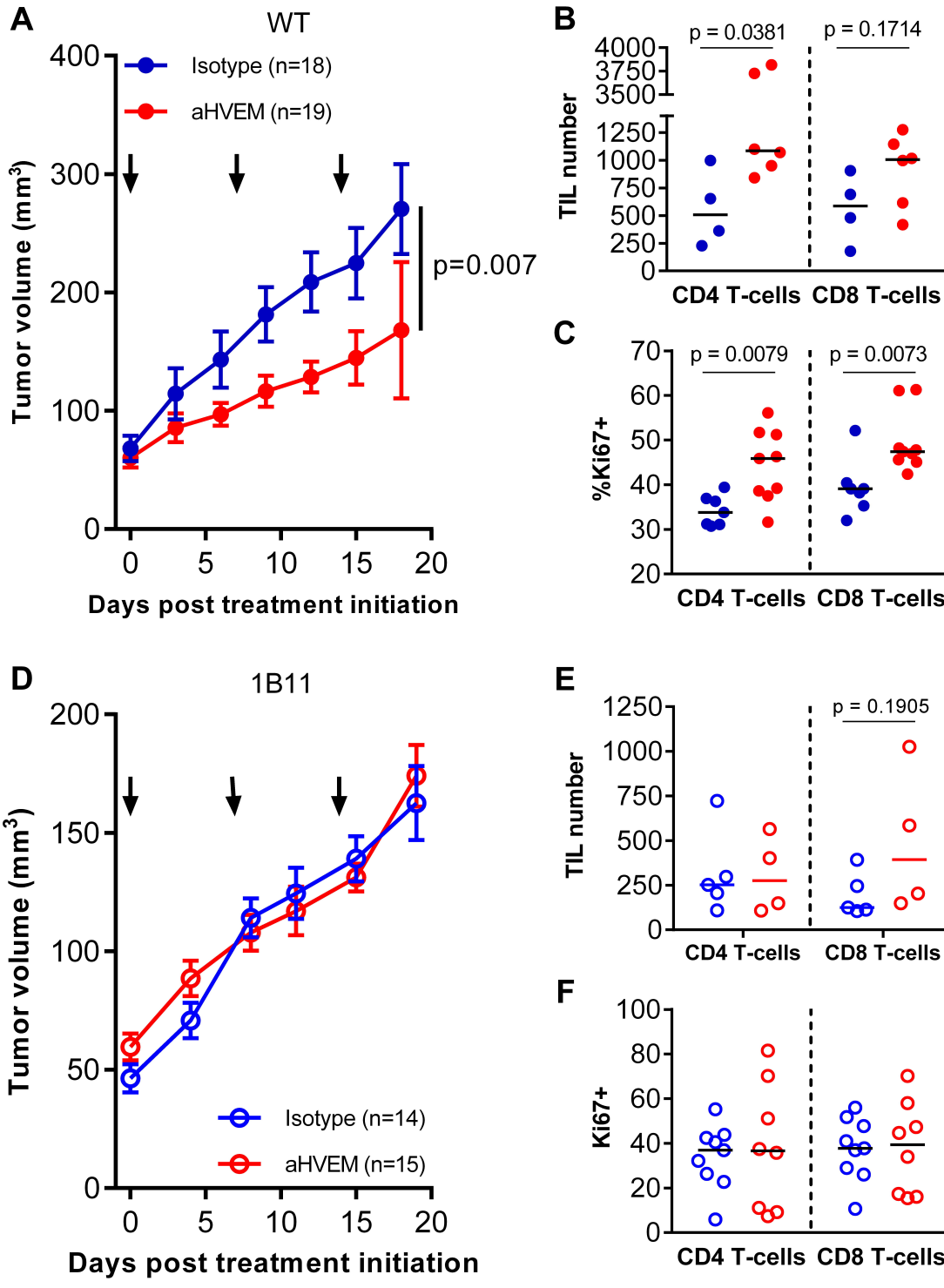
A
WT
Isotype (n=18)
aHVEM (n=19)
Tumor volume (mm3)
Days post treatment initiation
p=0.007
B
p = 0.0381
p = 0.1714
TIL number
CD4 T-cells
CD8 T-cells
C
p = 0.0079
p = 0.0073
%Ki67+
CD4 T-cells
CD8 T-cells
D
1B11
Isotype (n=14)
aHVEM (n=15)
Tumor volume (mm3)
Days post treatment initiation
E
p = 0.1905
TIL number
CD4 T-cells
CD8 T-cells
F
Ki67+
CD4 T-cells
CD8 T-cells

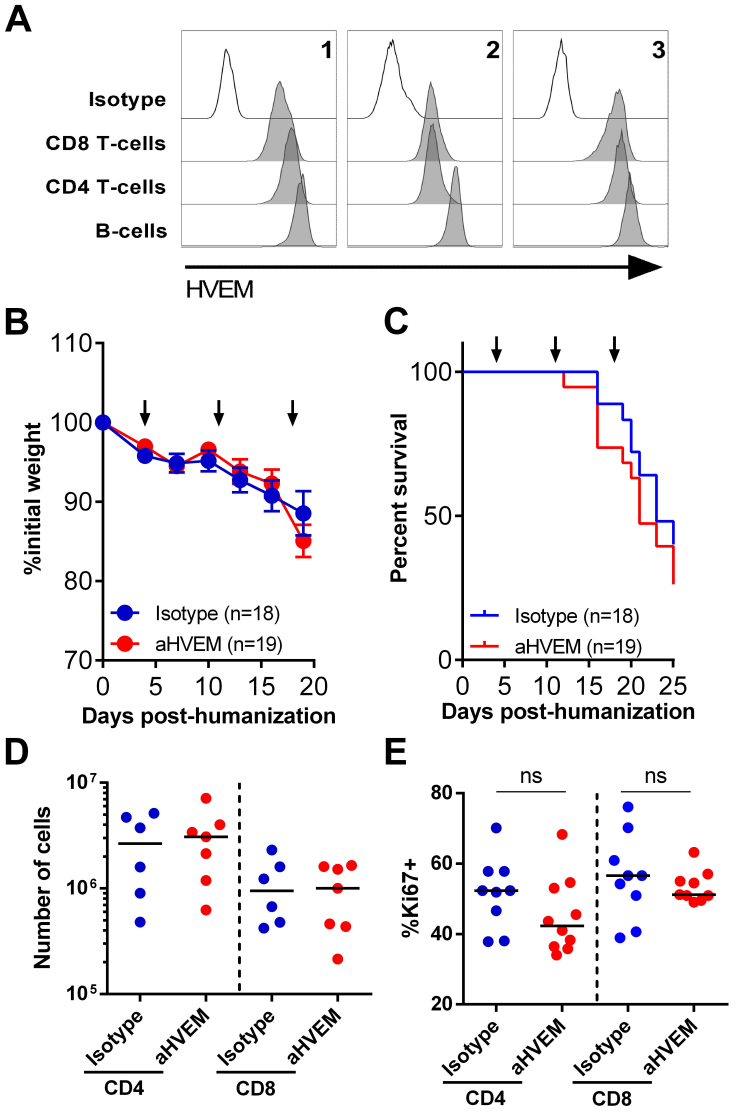
A
1
2
3
Isotype
CD8 T-cells
CD4 T-cells
B-cells
HVEM
B
%initial weight
110
100
90
80
70
0
5
10
15
20
Isotype (n=18)
aHVEM (n=19)
Days post-humanization
C
Percent survival
100
50
0
0
5
10
15
20
25
Isotype (n=18)
aHVEM (n=19)
Days post-humanization
D
Number of cells
10^7
10^6
10^5
Isotype
aHVEM
Isotype
aHVEM
CD4
CD8
E
%Ki67+
80
60
40
20
ns
ns
Isotype
aHVEM
Isotype
aHVEM
CD4
CD8

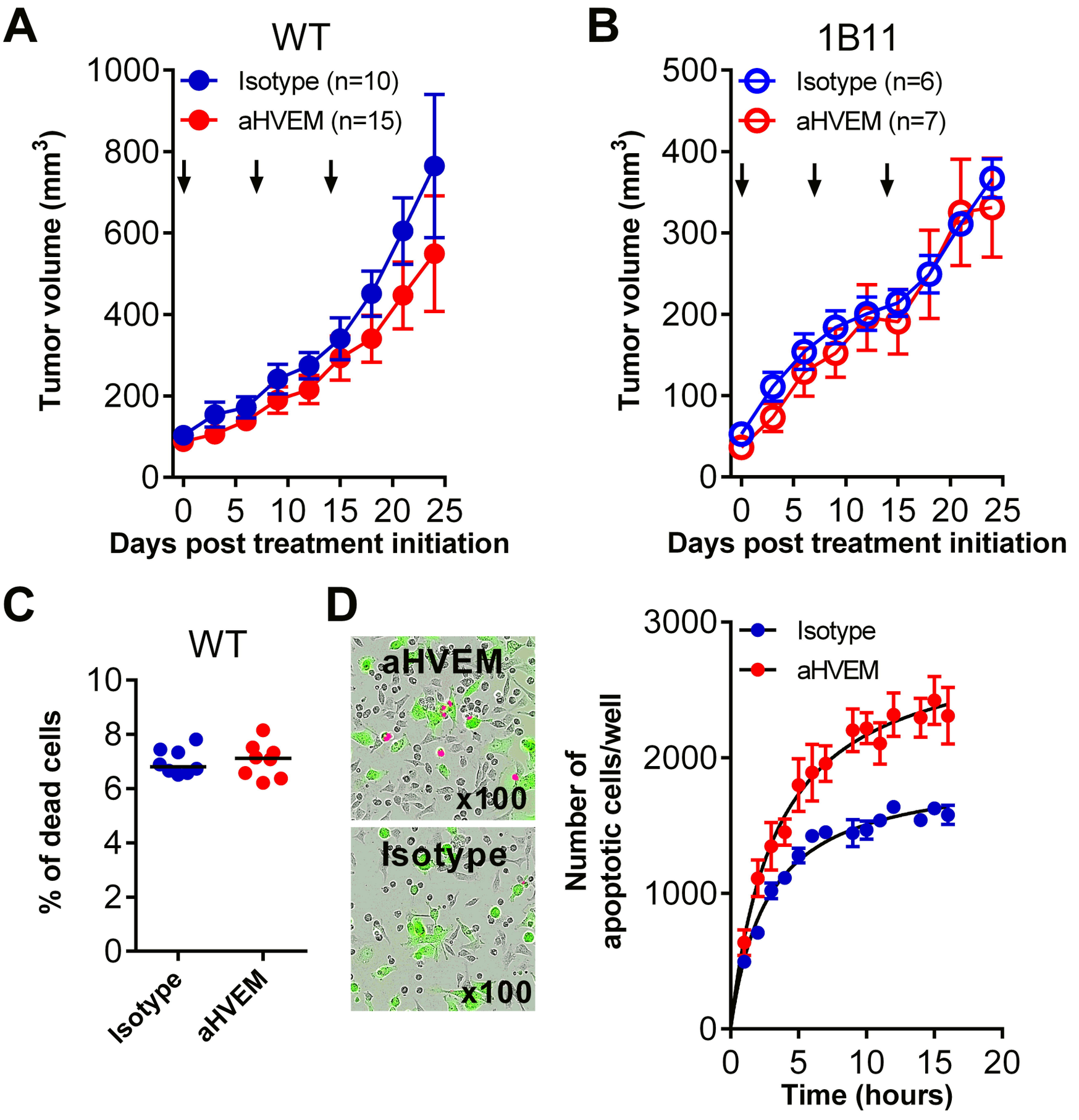
A
WT
Isotype (n=10)
aHVEM (n=15)
Tumor volume (mm3)
Days post treatment initiation
B
1B11
Isotype (n=6)
aHVEM (n=7)
Tumor volume (mm3)
Days post treatment initiation
C
WT
% of dead cells
Isotype
aHVEM
D
aHVEM
x100
Isotype
x100
Isotype
aHVEM
Number of apoptotic cells/well
Time (hours)

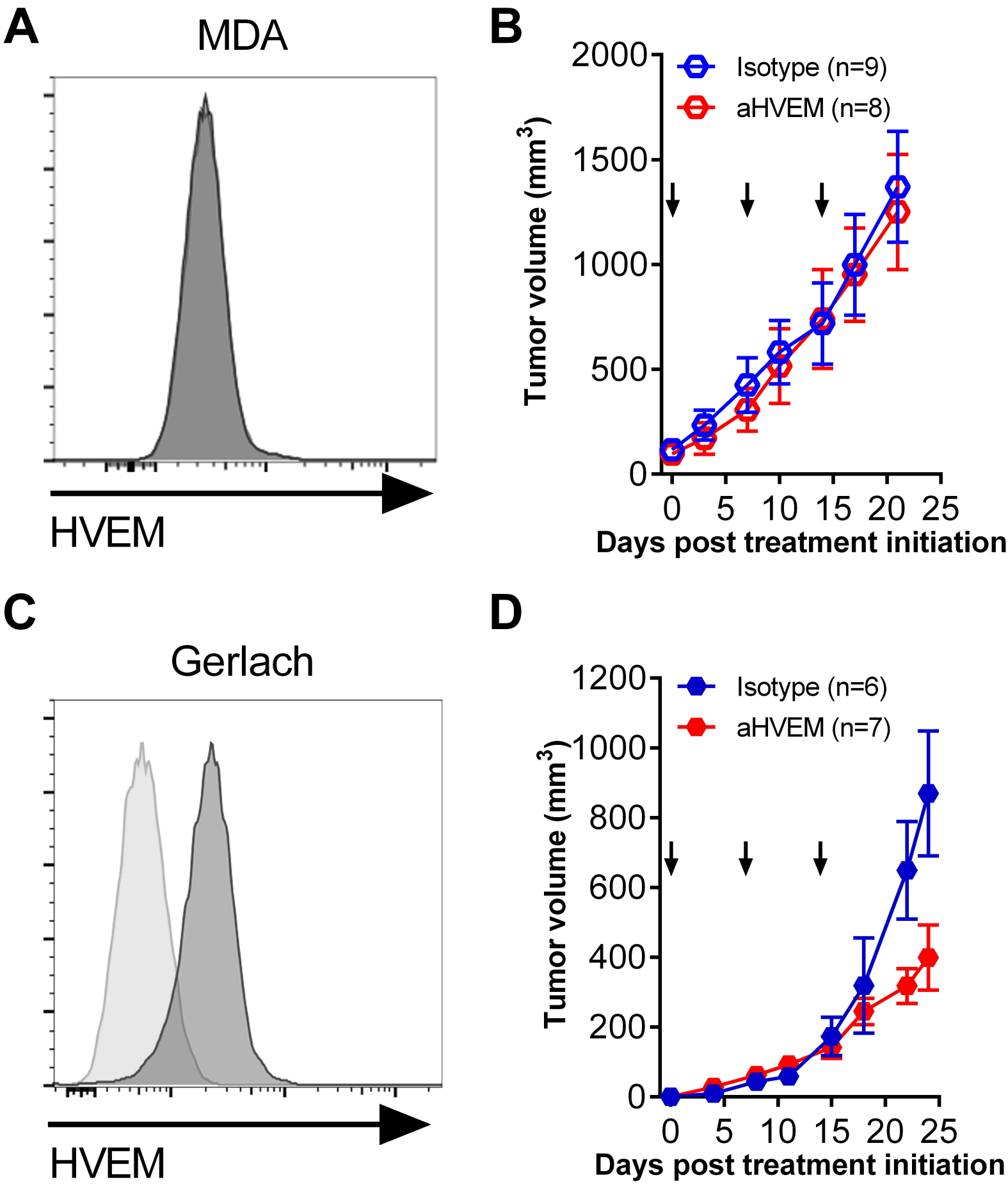
A
MDA
HVEM
B
Isotype (n=9)
aHVEM (n=8)
Tumor volume (mm3)
2000
1500
1000
500
0
0 5 10 15 20 25
Days post treatment initiation
C
Gerlach
HVEM
D
Isotype (n=6)
aHVEM (n=7)
Tumor volume (mm3)
1200
1000
800
600
400
200
0
0 5 10 15 20 25
Days post treatment initiation